Journal of Nuclear Medicine, published on August 3, 2017 as doi:10.2967/jnumed.117.196485

Clinical Molecular Imaging of Chemokine Receptor CXCR4 Expression in Atherosclerotic Plaque using ^{68}Ga-Pentixafor PET: Correlation with Cardiovascular Risk Factors and Calcified Plaque Burden

Desiree Weiberg, MD[1]; James T. Thackeray, PhD[1]; Guenter Daum, PhD[2]; Jan M. Sohns, MD[1]; Saskia Kropf[3]; Hans-Juergen Wester, PhD[4]; Tobias L. Ross, PhD[1]; Frank M. Bengel, MD[1]; Thorsten Derlin, MD[1*]

[1]Department of Nuclear Medicine, Hannover Medical School, Hannover, Germany,

[2]Department of Vascular Medicine, University Heart Center Hamburg-Eppendorf, Germany,

[3]Scintomics GmbH, Fürstenfeldbruck, Germany

[4]Pharmaceutical Radiochemistry, Technical University of Munich, Munich, Germany

***Corresponding author:**

Thorsten Derlin, M.D.
Department of Nuclear Medicine
Hannover Medical School
Carl-Neuberg-Str. 1
D-30625 Hannover, Germany
Tel.: +49 (0) 511 532 2577
Fax: +49 (0) 511 532 3761
E-mail: Derlin.Thorsten@mh-hannover.de

First author:

Desiree Weiberg, M.D.
Department of Nuclear Medicine
Hannover Medical School
Carl-Neuberg-Str. 1
D-30625 Hannover, Germany
Tel.: +49 (0) 511 532 2577
Fax: +49 (0) 511 532 3761
Weiberg.Desiree@mh-hannover.de

Short running title: Plaque Imaging Using ^{68}Ga-Pentixafor PET

Word count (Title Page, Abstract, Text, References, Figures, Tables): 5018

Word count (Abstract): 238

Tables: 4(+2Suppl.) **Figures:** 3

ABSTRACT

The CXC-motif chemokine receptor 4 (CXCR4) represents a promising target for molecular imaging of different CXCR4$^+$ cell types in cardiovascular diseases including atherosclerosis and arterial wall injury. The aim of this study was to assess the prevalence, pattern, and clinical correlates of arterial wall accumulation of ^{68}Ga-Pentixafor, a specific CXCR4 ligand for positron emission tomography (PET).

Methods: Data of fifty-one patients who underwent ^{68}Ga-Pentixafor PET/computed tomography (PET/CT) for non-cardiovascular indications were retrospectively analyzed. Tracer accumulation in the vessel wall of major arteries was analyzed qualitatively and semiquantitatively by blood-pool-corrected target-to-background ratios (TBRs). Tracer uptake was compared with calcified plaque burden and cardiovascular risk factors.

Results: Focal arterial uptake of ^{68}Ga-Pentixafor was seen at 1411 sites in 51 (100%) of patients. ^{68}Ga-Pentixafor uptake was significantly associated with calcified plaque burden (P<0.0001) and cardiovascular risk factors including age (P<0.0001), arterial hypertension (P<0.0001), hypercholesterolemia (P=0.0005), history of smoking (P=0.01), and prior cardiovascular events (P=0.0004). Both the prevalence (P<0.0001) and signal intensity (P=0.009) of ^{68}Ga-Pentixafor uptake increased as the number of risk factors increased.

Conclusion: ^{68}Ga-Pentixafor PET/CT is suitable for non-invasive, highly specific PET imaging of CXCR4 expression in the atherosclerotic arterial wall. Arterial wall ^{68}Ga-Pentixafor uptake is significantly associated with surrogate markers of atherosclerosis, and is linked to the presence of cardiovascular risk factors. ^{68}Ga-Pentixafor signal is

higher in patients with a high-risk profile, and may hold promise for identification of vulnerable plaque.

Key words: CXCR4; Atherosclerosis; Plaque; ^{68}Ga-Pentixafor; PET/CT

INTRODUCTION

CXCR4 and its ligand, CXCL12, play an important role in trafficking of progenitor and inflammatory cells (*1*). *Ex vivo* data have demonstrated a progressive accumulation of CXCR4$^+$ cells during plaque evolution (*1*). The role of the CXCR4/CXCL12 axis has recently been emphasized in models of ischemic injury (*2-6*). Of note, vulnerable plaque is characterized by distinct histopathological hallmarks, including a preponderance of inflammatory CXCR4$^+$ cells such as monocytes/macrophages (*1,7*). Furthermore, CXCR4 is also expressed by other leukocyte populations and, importantly, different cell types including smooth muscle cell (SMC) progenitors and endothelial progenitor cells contributing to plaque evolution (*1*). Therefore, we hypothesized that CXCR4 would be a suitable target for imaging of plaque pathophysiology.

PET has become a well-studied imaging technique for non-invasive molecular imaging of various aspects of atherosclerosis (*8*), e.g. for the quantification of macrophage-mediated inflammation in atherosclerotic lesions using ^{18}F-fluorodeoxyglucose (FDG) (*9,10*). However, ^{18}F-FDG exhibits several inherent limitations, including a nonspecific mechanism of uptake, physiologic uptake in brain and myocardium, interaction with blood glucose, and the requirement for a fasting period before imaging.

Recently, the highly specific radiotracer ^{68}Ga-Pentixafor has been introduced for clinical molecular imaging of CXCR4 expression (*11-14*). Our group has reported on the feasibility of ^{68}Ga-Pentixafor PET for non-invasive characterization of post-infarction myocardial inflammation. In mice after coronary artery ligation, CXCR4 up-regulation

was proportional to flow cytometry-derived elevation of $CD45^+$ leukocytes in the left ventricle and increased immunohistochemical detection of $CD68^+$ macrophages and $Ly6G^+$ granulocytes in the infarct territory (*5*). More recently, ^{68}Ga-Pentixafor PET detected CXCR4 expression by inflammatory cells present in atherosclerotic plaques of an experimental rabbit model, and in a limited patient cohort (*15*). Immunohistochemistry of human carotid plaques demonstrated CXCR4 expression localized to regions with high $CD68^+$ macrophage content (*15*).

However, experience with and interpretation of ^{68}Ga-Pentixafor PET imaging of arterial wall physiology in humans remain limited. Therefore, the purpose of the present study was to assess the prevalence, distribution, and topographic relationship of arterial lesions with increased ^{68}Ga-Pentixafor accumulation as determined by PET relative to arterial calcification as assessed by CT.

METHODS

Study Population

The study population of this retrospective study consisted of 51 patients (12 women, 39 men; mean age±standard deviation (SD), 59.5±16.2 years; range 22.7-85.0 years) who had been referred to our institution for a ^{68}Ga-Pentixafor PET/CT scan for various non-cardiovascular clinical indications (interstitial lung disease, n=21; sarcoidosis, n=13; complicated urinary tract infection, n=8; leukemia, n=5; miscellaneous, n=4) between February 2015 and June 2016. Gender, age (age at risk,

women: >55y, men: >45y) and other common cardiovascular risk factors including hypertension, hypercholesterolemia, diabetes, smoking habits, and prior vascular events defined as myocardial infarction or cerebrovascular insult were documented for each patient (*16*). Risk factors were considered categoric variables. Because of the potential influence of statins on plaque physiology and on expression of CXCR4 on monocytes, treatment with statins was also recorded (*17*). Exclusion criteria were: history of vasculitis, chemotherapy in the preceding 4 weeks, cardiovascular event in the preceding 6 months. The protocol complied with the Declaration of Helsinki. The institutional review board approved this retrospective study, and the requirement to obtain informed consent was waived.

Radiolabeling of ^{68}Ga-Pentixafor, Image Acquisition and Reconstruction

Material for synthesis of ^{68}Ga-Pentixafor (CPCR4.2) was provided by Scintomics (Fürstenfeldbruck, Germany). Synthesis was performed using a cold mass of 15 nmol CPCR4.2, and a 1.11 GBq ^{68}Ge/^{68}Ga-generator (Eckert&Ziegler, Berlin, Germany) connected to a Scintomics good radiopharmaceutical practice synthesis module, as described previously (*12-14,18*).

All studies were obtained on a dedicated PET/CT system (Siemens Biograph mCT 128 Flow; Siemens Knoxville, TN) equipped with an extended field-of-view PET component, a 128-slice spiral CT component and a magnetically driven table optimized for continuous scanning. ^{68}Ga-Pentixafor was injected intravenously at a dose of 123±32 MBq. After an uptake period of 60 minutes, imaging started with a single low-dose non-

enhanced helical CT (120kV, mA modulated, pitch 1.2, reconstructed axial slice thickness 5.0 mm) performed for attenuation correction of PET acquisitions. Whole-body PET images were then acquired in all patients using continuous bed motion at a speed of 2.0 mm/s for head, 0.5 mm/s for chest and abdomen and 2.5 mm/s for legs. All studies were reconstructed using time-of-flight and point-spread function TrueX information combined with an iterative algorithm (Ultra HD®, Siemens Healthcare; 2 iterations, 21 subsets, matrix 200; zoom 1.0; Gaussian filter of 2.0).

Image Analysis

Transaxial PET, CT and fused PET/CT ^{68}Ga-Pentixafor images were analyzed both visually and semiquantitatively on a dedicated workstation (syngo.via; V10B; Siemens Healthcare, Erlangen, Germany). The scans were analyzed on the basis of patients, arterial segments and lesions. For segment-based analysis, the major arteries were subdivided as follows: right and left common carotid arteries, thoracic aorta, abdominal aorta, right and left iliac as well as right and left femoral arteries.

Calcified Plaque (CP). CPs were defined as high-density mural areas (attenuation > 130 Hounsfield units) in the wall of the studied arteries (*19*). First, CT images were visually analyzed for the presence of CPs. Patients were divided into those with CP (CT+) and those without discernible CP (CT-). The calcified lesion thickness defined as the maximum calcification diameter measured in the intimo-adventitial direction was measured. Each arterial segment was classified on a five-point-scale for grading the maximum circumferential extent of calcifications: 0, absent; 1, less than 25% of arterial

wall circumference; 2, 25%–50% of arterial wall circumference; 3, 50%–75% of arterial wall circumference; and 4, greater than 75% of arterial wall circumference (*16*).

Radiotracer Uptake. PET images were visually evaluated for the presence of focal radiotracer uptake above background signal in arterial walls (PET positive, PET+). The localization of PET positive lesions in relation to CPs and the vascular wall was analyzed in PET/CT fusion images. Semiquantitative analysis was performed by obtaining the maximum standardized uptake value (SUV_{max}) of a lesion by manually placing an individual 3D volume-of-interest (typically 10 mm in diameter) around the lesion on coregistered transaxial PET/CT images. Blood-pool SUV ($SUV_{blood\text{-}pool}$) was measured as mean from 3 regions of interest of fixed size (10 mm) placed in the mid lumen of the superior vena cava. For the calculation of the arterial TBR, the SUV of each arterial lesion was divided by the $SUV_{blood\text{-}pool}$ (*10*).

Statistical Analysis

Continuous variables are expressed as mean ± SD. Categoric variables are presented with absolute and relative frequencies. For between-group comparisons of parametric continuous data, *P* values were calculated from an unpaired Student`s *t* test. The Pearson correlation coefficient *r* was used to assess the relationship between PET and CT findings as well as imaging findings and cardiovascular risk factors. Afterwards, a stepwise multiple regression analysis was performed to determine an independent association between the imaging findings (Number of CP, number of PET+ foci, TBR) and cardiovascular risk factors. TBR divided into quartiles was analyzed using one-way

analysis of variance. Statistical significance was established for *P* values of less than 0.05. Statistical analysis was performed using GraphPad Prism (Version 6.0 for Mac OS X [Apple]; Graphpad Software Inc., San Diego, USA) and MedCalc Statistical Software version 17.1 (MedCalc Software, Ostend, Belgium).

RESULTS

^{68}Ga-Pentixafor uptake measurements and the assessment of CP burden were feasible in all patients. Relevant clinical patient characteristics are reported in **Table 1**.

Arterial Wall ^{68}Ga-Pentixafor Uptake and CP Burden

Focally increased ^{68}Ga-Pentixafor uptake in the arterial wall (**Table 2**) was observed at 1411 sites in 51 (100%) patients. The prevalence of uptake was the highest in the abdominal aorta, followed by the thoracic aorta. Mean SUV_{max} was 3.4±0.7, and values ranged from 1.8 to 7.3. Mean $SUV_{blood\text{-}pool}$ was 1.8±0.3, and values ranged from 1.2 to 2.6. Mean TBR was 2.0±0.5, and values ranged from 1.1 to 4.9. TBR was also highest in the abdominal aorta.

Calcified atherosclerotic lesions (**Table 3**) were detected at 6456 sites in 42 (82.4%) of the 51 study patients. On average, 24.1±25.4 (range, 1 to 125) calcified plaques were found in each arterial segment with observable calcification, and the

abdominal aorta showed the highest CP burden. Mean calcification thickness was 2.8±1.3 mm (range, 1 to 8 mm).

Relationship between ^{68}Ga-Pentixafor Uptake, CP Burden, and Cardiovascular Risk Factors

On a per-patient basis, 51 (100%) patients were PET+, whereas 42 (82.4%) patients were CT+. 42 (82.4%) patients were PET+/CT+, 9 (17.6%) patients were PET+/CT-.

On a per-segment basis, 330 (80.9%) of the 408 studied arterial segments were ^{68}Ga-Pentixafor PET+, and 268 (65.7%) were CT+. There were on average 4.2 ± 3.3 (range, 1-16) sites of ^{68}Ga-Pentixafor uptake in an affected segment, and 24.1 ± 25.4 (range, 1-125) calcified lesions.

On a per-lesion basis, 473 (33.5%) of the 1411 arterial lesions with radiotracer accumulation showed concordant calcification. Only 7.3% of all arterial calcification sites showed increased ^{68}Ga-Pentixafor uptake (**Figs. 1** and **2)**. Consistent with these findings, there was a statistically significant correlation between the number of PET+ arterial uptake sites and CP burden (r=0.67, P<0.0001), maximum plaque thickness (r=0.56, P<0.0001) and calcification score (r=0.69, P<0.0001), all describing different aspects of the extent of arterial calcification.

On average, study patients had 4±2 (range, 1-7) cardiovascular risk factors. A significant correlation was found between the number of cardiovascular risk factors per patient and the number of calcified plaques (r=0.46, P=0.0007), the number of PET+ lesions (r=0.70, P<0.0001), and TBR (r=0.36, P=0.009) (**Fig. 3**). Single variable

regression analysis demonstrated significant correlations between the number of PET+ arterial lesions and age at risk (r=0.60, P<0.0001), arterial hypertension (r=0.56, P<0.0001), hypercholesterolemia (r=0.47, P=0.0005), history of smoking (r=0.35, P=0.01), and prior vascular events (r=0.47, P=0.0004) (**Supplemental Table 1**). Multiple regression analysis revealed age at risk (r=0.50, P=0.0003), arterial hypertension (r=0.52, P=0.0001) and history of smoking (r=0.36, P=0.01) were independently associated with PET+ arterial lesions (**Supplemental Table 2**).

Regarding the relationship of CP and cardiovascular risk factors, a significant correlation between CP burden and age at risk (r=0.51, P=0.0001), the presence of arterial hypertension (r=0.37, P=0.008) and prior vascular events (r=0.46, P=0.0008) was observed. Multiple regression analysis showed independent association between CP burden and age at risk (r=0.49, P=0.0003) and prior vascular events (r=0.38, P=0.008).

Both the number of arterial uptake sites and CP burden were significantly associated with current statin therapy (P<0.0001 and P=0.0009, respectively). TBR was not significantly different between patients with (2.7±0.8) or without (2.5±0.8) ongoing statin treatment (P=0.23).

DISCUSSION

To our knowledge, this is the first study that reports on the prevalence, pattern, and clinical correlates of arterial wall accumulation of ^{68}Ga-Pentixafor in large arteries of

patients, and establishes ^{68}Ga-Pentixafor PET/CT for imaging of CXCR4 expression in the atherosclerotic vessel wall. This novel methodology may refine the characterization of atherosclerotic lesions and may serve as a platform for future clinical studies targeting CXCR4$^+$ cells in atherosclerosis.

The CXCR4/CXCL12 axis (**Table 4**) plays a pivotal role in atherosclerosis and arterial injury (*1,20*). In advanced plaque, the density of macrophages indicates the risk of an atherothrombotic event as macrophages release proteolytic enzymes degrading the fibrous cap and promote the intralesional inflammation by secreting pro-inflammatory cytokines (*8*). Therefore, many commonly used tracers including ^{18}F-FDG and ^{68}Ga-DOTATATE are used to visualize different aspects of macrophage density, the latter with limited success (*8,21*). Previous immunohistochemical analyses of CXCR4 expression in human atherosclerotic plaque revealed a progressive accumulation of CXCR4$^+$ cells during plaque evolution, and CXCR4$^+$ leukocytes have been detected in culprit lesions in acute coronary syndromes (*22*). Taken together, CXCR4 expression by leukocytes is associated with vulnerability of plaque. Indeed, vascular ^{68}Ga-Pentixafor uptake showed a marked independent association with established risk factors such as age at risk (r=0.50, P=0.0003), arterial hypertension (r=0.52, P=0.0001) and history of smoking (r=0.36, P=0.01). More importantly, both the number of CXCR4$^+$ lesions (r=0.70, P<0.0001) and TBR (r=0.36, P=0.009) increased as the number of risk factors increased, suggesting a role for identifying risk-bearing atherosclerotic plaques.

Hyafil and colleagues have recently reported that CXCR4 expression is associated with CD68$^+$ macrophage-rich areas on immunohistochemistry of human

carotid plaques (*15*). Additionally, atherosclerotic plaques were induced by endothelial abrasion of large arteries in rabbits fed with an atherogenic diet in that work, leading to macrophage-riche plaques which were subsequently found to be CXCR4$^+$ (*15*). However, results from this non-physiological model of atherosclerotic plaque requiring both a considerable arterial injury and a special atherogenic diet may not be easily translated into the human clinical setting in which atherogenic factors are much less pronounced, inflammation is not artificially induced and less macrophage–dominated, and a variety of physiological mechanisms are involved in the evolution of plaque. Indeed, other cell types involved in plaque evolution including SMC progenitors and endothelial progenitor cells have also been found to express CXCR4 (*1*). Importantly, CXCR4 is also expressed by mature endothelial and SMCs in the arterial wall (*1*), indicating that other cell types may relevantly contribute to the *in vivo* CXCR4 signal. Arterial injury has been demonstrated to induce local SMC CXCR4 expression, contributing to intimal hyperplasia (*23*). This indicates that a portion of ^{68}Ga-Pentixafor uptake could reflect mechanisms other than atherosclerosis, e.g. arterial injury in areas of turbulent flow. Finally, it has recently been shown that both CXCR4$^+$ endothelial cells and SMCs are atheroprotective in an apolipoprotein E-deficient mouse model, limiting atherosclerosis by maintaining arterial integrity and preserving endothelial barrier function (*24*). This underlines that CXCR4$^+$ cells have many different roles both in the atherosclerotic and in the non-atherosclerotic arterial wall (*1*). Although our results indicate a potential role of ^{68}Ga-Pentixafor PET/CT as a tool not only for *in vivo* visualization of CXCR4$^+$ atherosclerotic lesions in the large arteries, but also for identification of inflamed, rupture-prone plaques, the relative contribution of different

pathophysiologic mechanisms and different cell types to the observed CXCR4 signal still remains to be elucidated.

Of note, the ^{18}F-FDG signal in atherosclerotic lesions may be attenuated by use of statins. Likely due to the high cardiovascular risk profile, the number of arterial uptake sites and CP burden were higher in patients receiving statin treatment. However, the signal intensity (TBR) did not differ significantly in patients with or without ongoing statin treatment (P=0.23). These results are supported by recent data which found no significant impact of incubation with statins on CXCR4 expression by macrophages (*15*), although other studies suggested some effect in certain monocyte subsets (*17*).

When analyzing the TBR of ^{68}Ga-Pentixafor, a good contrast between atherosclerotic lesions and the blood-pool was found. The mean TBR of 2.0±0.5 of CXCR4$^+$ lesions is comparable to the TBR of ^{18}F-sodium fluoride and even higher than the TBR of ^{18}F-FDG, facilitating the identification of atherosclerotic lesions (*10,16,25,26*). The tracer distribution of ^{68}Ga-Pentixafor throughout the major arteries was consistent with established atherosclerotic topography (*25-27*).

Although ^{68}Ga-Pentixafor uptake was observed in all patients, CPs were less common (17.6% PET+/CT- patients). Interestingly, these patients were considerably younger than PET+/CT+ patients (34.6 ± 8.8 vs 64.9 ± 11.8 years), suggesting that the presence of CXCR4$^+$ cells begins at an early age and precedes arterial calcification. In consistence with that observation, only 7.3% of all arterial calcification sites showed ^{68}Ga-Pentixafor accumulation. Calcified plaque is usually considered stable, late-stage atherosclerotic disease, underlining that CXCR4 imaging may identify earlier stages of

plaque development, and non-stable vulnerable plaque. Indeed, CXCR4$^+$ cells are involved in the initiation, progression and rupture of atherosclerotic plaque (*1,7*). ^{18}F-FDG uptake representing a measure of macrophage density in plaque is likewise rarely seen in calcified plaque (*10,26*). Furthermore, ^{68}Ga-Pentixafor uptake is clearly linked to the clinical cardiovascular risk profile, supporting a role for identifying risk-bearing plaque. The rate of colocalization between vascular ^{68}Ga-Pentixafor accumulation and calcification was 33.5%, while for ^{18}F-FDG coincident calcification was reported less frequently (*10,26*). These results indicate that CXCR4-targeted imaging may identify additional CXCR4$^+$ cells in the arterial wall besides intralesional macrophages which represent the vascular target of ^{18}F-FDG PET. Indeed, CXCR4 is also expressed by a variety of progenitor and other cells in the arterial wall, including endothelial and vascular smooth muscle cells (*1*).

Some limitations of the present study should be acknowledged. First, the precise cell type contributing to the in vivo ^{68}Ga-Pentixafor signal cannot be identified. However, previous *ex vivo* data evidenced up-regulated CXCR4 expression by macrophages in atherosclerotic lesions (*15*). Second, the results of this study might not be perfectly generalizable to other patient populations. However, factors that might affect physiological processes in the vessel wall were carefully excluded. Second, scans were performed using a routine imaging protocol for ^{68}Ga-Pentixafor imaging optimized for other indications. Dynamic or delayed data acquisition may provide additional information for the assessment of atherosclerotic plaques (*28*). ^{68}Ga-Pentixafor exhibits a relatively high blood-pool signal. However, at least some part of that signal is caused by specific binding of ^{68}Ga-Pentixafor on CXCR4$^+$ cells, questioning the potential impact

of delayed imaging which will rather support renal elimination of unbound tracer. In addition, the positron range for ^{68}Ga is much higher than for ^{18}F, potentially affecting the localization of the vessel wall signal and contributing to partial volume effects. Given the fact that (i) Pentixafor is a specific marker of CXCR4^{+} cell infiltration, (ii) there are numerous preclinical studies linking plaque progression and CXCR4, and (iii) established cardiovascular risk factors were strongly associated with tracer uptake in this study, we hypothesize that CXCR4-targeted PET imaging bears promise to stratify the risk of impending atherothrombotic events.

Conclusion

On the basis of *ex vivo* findings of CXCR4 expression in atherosclerotic plaque, the present study demonstrates that ^{68}Ga-Pentixafor PET/CT is suitable for non-invasive, highly specific clinical PET imaging of CXCR4 expression in the atherosclerotic wall of large arteries. ^{68}Ga-Pentixafor uptake is significantly associated with calcified plaque burden and cardiovascular risk factors, and may hold promise for identification of vulnerable plaque. This study provides a rationale to incorporate ^{68}Ga-Pentixafor PET into further preclinical and clinical studies to obtain new insights into CXCR4 expression in atherosclerotic lesions and to evaluate whether it may be used to specifically monitor interventions targeting CXCR4.

Disclosure

Saskia Kropf is CEO of Scintomics. Dr. Hans-Jürgen Wester is shareholder of Scintomics. No other potential conflict of interest relevant to this article was reported.

Acknowledgments

None.

REFERENCES

1. Döring Y, Pawig L, Weber C, Noels H. The CXCL12/CXCR4 chemokine ligand/receptor axis in cardiovascular disease. *Front Physiol.* 2014;5:212.

2. Ceradini DJ, Kulkarni AR, Callaghan MJ, et al. Progenitor cell trafficking is regulated by hypoxic gradients through HIF-1 induction of SDF-1. *Nat Med.* 2004;10:858–864.

3. Lim CS, Kiriakidis S, Sandison A, Paleolog EM, Davies AH. Hypoxia-inducible factor pathway and diseases of the vascular wall. *J Vasc Surg.* 2013;58:219-230.

4. Petit I, Jin D, Rafii S. The SDF-1–CXCR4 signaling pathway: a molecular hub modulating neo-angiogenesis. *Trends Immunol.* 2007;28:299–307.

5. Thackeray JT, Derlin T, Haghikia A, et al. Molecular imaging of the chemokine receptor CXCR4 after acute myocardial infarction. *JACC Cardiovasc Imaging.* 2015;8:1417-1426.

6. Lapa C, Reiter T, Werner RA, et al. [(68)Ga]Pentixafor-PET/CT for imaging of chemokine receptor 4 expression after myocardial infarction. *JACC Cardiovasc Imaging.* 2015;8:1466-1468.

7. Gupta SK, Pillarisetti K, Lysko PG. Modulation of CXCR4 expression and SDF-1 alpha functional activity during differentiation of human monocytes and macrophages. *J Leukoc Biol.* 1999;66:135–143.

8. Joseph P, Tawakol A. Imaging atherosclerosis with positron emission tomography. *Eur Heart J.* 2016;37:2974-2980.

9. Tarkin JM, Dweck MR, Evans NR, et al. Imaging atherosclerosis. *Circ Res.* 2016;118:750-769.

10. Derlin T, Tóth Z, Papp L, et al. Correlation of inflammation assessed by ^{18}F-FDG PET, active mineral deposition assessed by ^{18}F-fluoride PET, and vascular calcification in atherosclerotic plaque: a dual-tracer PET/CT study. *J Nucl Med.* 2011;52:1020-1027.

11. Gourni E, Demmer O, Schottelius M, et al. PET of CXCR4 expression by a (68)Ga-labeled highly specific targeted contrast agent. *J Nucl Med.* 2011;52:1803-1810.

12. Wester HJ, Keller U, Schottelius M, et al. Disclosing the CXCR4 expression in lymphoproliferative diseases by targeted molecular imaging. *Theranostics*. 2015;5:618-630.

13. Herrmann K, Lapa C, Wester HJ, et al. Biodistribution and radiation dosimetry for the chemokine receptor CXCR4-targeting probe ^{68}Ga-pentixafor. *J Nucl Med.* 2015;56:410-416.

14. Philipp-Abbrederis K, Herrmann K, Knop S, et al. In vivo molecular imaging of chemokine receptor CXCR4 expression in patients with advanced multiple myeloma. *EMBO Mol Med.* 2015;7:477-487.

15. Hyafil F, Pelisek J, Laitinen I, et al. Imaging the cytokine receptor CXCR4 in atherosclerotic plaques with the radiotracer ^{68}Ga-pentixafor for positron emission tomography. *J Nucl Med.* 2017;58:499-506.

16. Derlin T, Wisotzki C, Richter U, et al. In vivo imaging of mineral deposition in carotid plaque using ^{18}F-sodium fluoride PET/CT: correlation with atherogenic risk factors. *J Nucl Med.* 2011;52:362-368.

17. Jaipersad AS, Shantsila E, Blann A, Lip GY. The effect of statin therapy withdrawal on monocyte subsets. *Eur J Clin Invest.* 2013;43:1307-1313.

18. Demmer O, Gourni E, Schumacher U, et al. PET imaging of CXCR4 receptors in cancer by a new optimized ligand. *ChemMedChem*. 2011;6:1789-1791.

19. de Weert TT, Ouhlous M, Meijering E, et al. In vivo characterization and quantification of atherosclerotic carotid plaque components with multidetector computed tomography and histopathological correlation. *Arterioscler Thromb Vasc Biol.* 2006;26:2366-2372.

20. Weber C, Noels H. Atherosclerosis: current pathogenesis and therapeutic options. *Nat Med.* 2011;17:1410–1422.

21. Wan MYS, Endozo R, Michopoulou S, et al. PET/CT imaging of unstable carotid plaque with 68Ga-labeled somatostatin receptor ligand. *J Nucl Med.* 2017;58:774-790.

22. Naruko T, Ueda M, Haze K, et al. Neutrophil infiltration of culprit lesions in acute coronary syndromes. *Circulation.* 2002;106:2894-2900.

23. Shi X, Guo LW, Seedial S, et al. Local CXCR4 upregulation in the injured arterial wall contributes to intimal hyperplasia. *Stem Cells.* 2016;34:2744-2757.

24. Döring Y, Noels H, van der Vorst EPC, et al. Vascular CXCR4 limits atherosclerosis by maintaining arterial integrity: evidence from mouse and human studies. *Circulation.* April 27, 2017 [Epub ahead of print].

25. Derlin T, Richter U, Bannas P, et al. Feasibility of ^{18}F-sodium fluoride PET/CT for imaging of atherosclerotic plaque. *J Nucl Med.* 2010;51:862-865.

26. Dunphy MPS, Freiman A, Larson SM, Strauss HW. Association of vascular ^{18}F-FDG uptake with vascular calcification. *J Nucl Med.* 2005;46:1278–1284.

27. Derlin T, Habermann CR, Lengyel Z, et al. Feasibility of ^{11}C-acetate PET/CT for imaging of fatty acid synthesis in the atherosclerotic vessel wall. *J Nucl Med.* 2011;52:1848–1854.

28. Blomberg BA, Thomassen A, Takx RA, et al. Delayed ^{18}F-fluorodeoxyglucose PET/CT imaging improves quantitation of atherosclerotic plaque inflammation: results from the CAMONA study. *J Nucl Cardiol*. 2014;21:588-597.

FIGURES

Figure 1 ^{68}Ga-Pentixafor-PET/CT images of abdominal aorta in a 64-year-old man. Transaxial CT (**A**) and fused PET/CT (**B**) images showing ^{68}Ga-Pentixafor uptake in a calcified atherosclerotic lesion (*arrows*) coincident with calcification. **C**, **D** - coronal views

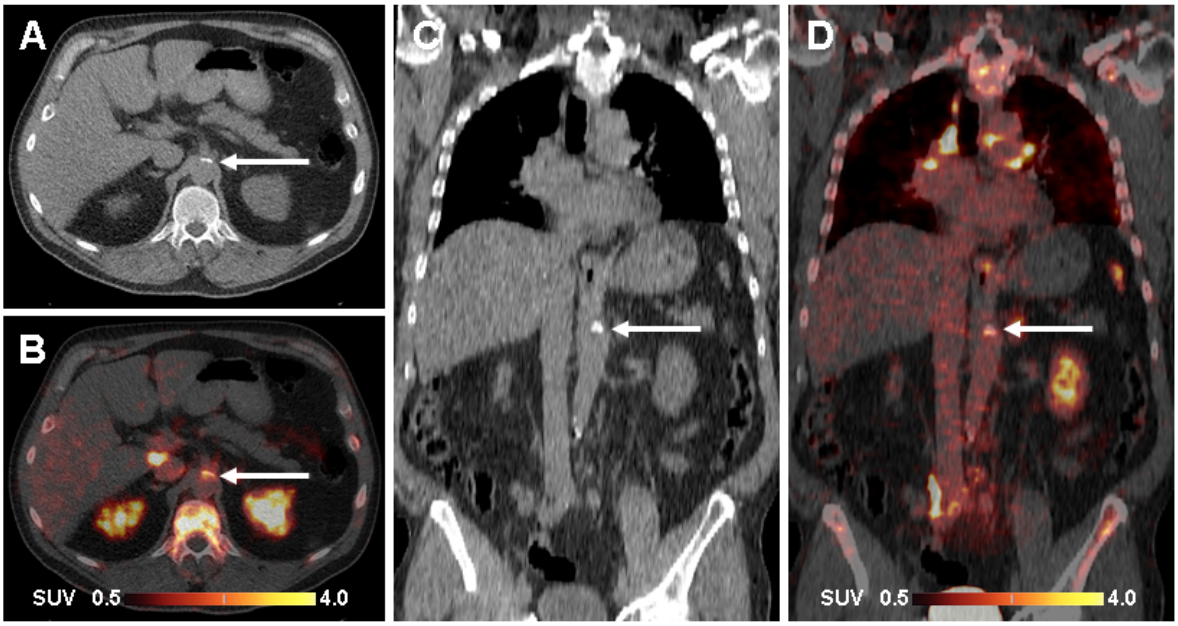

Figure 2 ^{68}Ga-Pentixafor-PET/CT images of abdominal aorta in a 64-year-old woman. (**A**) Transaxial CT image and (**B**) fused PET/CT image showing ^{68}Ga-Pentixafor uptake in a partly calcified atherosclerotic lesion (*arrow*) in the wall of an atherosclerotic ectatic aorta. Sagittal CT image (**C**) and fused PET/CT image (**D**) showing additional foci of ^{68}Ga-Pentixafor uptake in non-calcified plaque (*non-continuous arrow).*

Figure 3 Correlation between imaging findings and the number of cardiovascular risk factors. The number of CXCR4^{+} lesions (**A**), TBR (**B**) and the number of calcified plaques (**C**) significantly increase as the number of cardiovascular risk factors increases. TBR grouped to quartiles demonstrates high-risk profile in patients with high arterial CXCR4 expression (**D**).

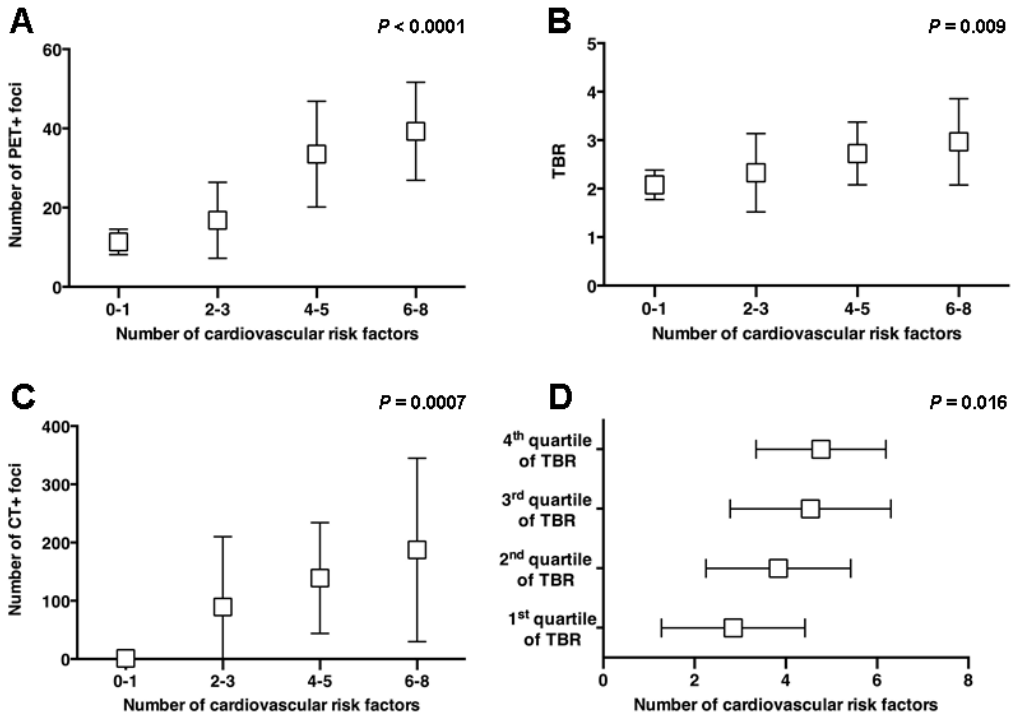

TABLES

Table 1 Patient characteristics of study population (*n=51*).

	CT+	PET+	PET+/CT+	PET+/CT-	Total study population
Subjects (n)	42	51	42	9	51
Age					
Mean ± SD	64.9 ± 11.8	59.5 ± 16.2	64.9 ± 11.8	34.6 ± 8.8	59.5 ± 16.2
Range	26.8 - 85.0	22.7 - 85.0	26.8 - 85.0	22.7 - 50.4	22.7 - 85.0
Age at risk	31 (73.8%)	39 (76.5%)	31 (73.8%)	8 (88.9%)	39 (76.5%)
Male gender	32 (76.2%)	39 (76.5%)	32 (76.2%)	7 (77.8%)	39 (76.5%)
Cardiovascular risk factors					
Hypertension (%)	29 (69.0%)	32 (62.7%)	29 (69.0%)	3 (33.0%)	32 (62.7%)
Hypercholesterolemia (%)	21 (50.0%)	22 (43.1%)	21 (50.0%)	1 (11.0%)	22 (43.1%)
Diabetes mellitus (%)	9 (21.4%)	10 (19.6%)	9 (21.4%)	1 (11.0%)	10 (19.6%)
History of smoking (%)	33 (78.6%)	38 (74.5%)	33 (78.6%)	5 (55.6%)	38 (74.5%)
Prior vascular event (%)	11 (26.2%)	11 (21.6%)	11 (26.2%)	0 (0.0%)	11 (21.6%)
Statin medication (%)	16 (38.1%)	17 (33.3%)	16 (38.1%)	1 (11.0%)	17 (33.3%)

Table 2 Prevalence, distribution and intensity of ^{68}Ga-Pentixafor uptake in the studied arteries.

	Right common carotid artery	Left common carotid artery	Thoracic aorta	Abdominal aorta	Right iliac arteries	Left iliac arteries	Right femoral arteries	Left femoral arteries	Total
Number (%) of patients with ^{68}Ga-Pentixafor uptake in the artery wall	30 (58.8%)	27 (52.9%)	50 (98.0%)	50 (98.0%)	43 (84.3%)	42 (82.4%)	44 (86.3%)	44 (86.3%)	51 (100.0%)
Total number (%) of uptake sites	49 (3.5%)	55 (3.9%)	339 (24.0%)	369 (26.2%)	115 (8.2%)	115 (8.2%)	180 (12.8%)	189 (13.4%)	1411 (100.0%)
Colocalization with calcification (%)	14 (28.6%)	15 (27.3%)	43 (12.7%)	156 (42.3%)	49 (42.6%)	53 (46.1%)	70 (38.9%)	73 (38.6%)	473 (33.5%)
SUV_{max}									
Mean ± SD	2.9 ± 0.5	2.9 ± 0.5	3.3 ± 0.6	3.6 ± 0.8	3.4 ± 0.7	3.4 ± 0.6	3.3 ± 0.6	3.4 ± 0.7	3.4 ± 0.7
Range	2.2 - 4.5	2.3 - 4.9	2.0 - 6.1	1.8 - 7.3	2.4 - 5.3	2.0 - 5.3	2.0 - 5.4	1.9 - 6.6	1.8 - 7.3
TBR									
Mean ± SD	1,7 ± 0,4	1.6 ± 0.4	1.9 ± 0.4	2.1 ± 0.6	1.9 ± 0.4	2.0 ± 0.5	1.9 ± 0.5	2.1 ± 0.6	2.0 ± 0.5
Range	1.1 - 2.8	1.1 - 2.9	1.2 - 4.3	1.2 - 4.9	1.2 - 3.1	1.2 - 3.9	1.2 - 4.3	1.2 - 4.4	1.1 - 4.9

Table 3 Prevalence, distribution and extent of calcification in the studied arteries.

	Right common carotid artery	Left common carotid artery	Thoracic aorta	Abdominal aorta	Right iliac arteries	Left iliac arteries	Right femoral arteries	Left femoral arteries	Total
No. (%) of patients with calcification sites	25 (49.0%)	23 (45.1%)	36 (70.6%)	40 (78.4%)	39 (76.5%)	35 (68.6%)	35 (68.6%)	35 (68.6%)	42 (82.4%)
No. (%) of calcification sites	175 (2.7%)	135 (2.1%)	891 (13.8%)	1735 (26.9%)	706 (10.9%)	615 (9.5%)	1119 (17.3%)	1080 (16.7%)	6456 (100%)
No. of calcification sites per affected segment									
Mean ± SD	7.0 ± 5.2	5.9 ± 4.0	24.8 ± 23.5	43.4 ± 33.8	18.1 ± 14.6	17.6 ± 13.4	32.0 ± 29.5	30.9 ± 28.4	24.1 ± 25.4
Range	1 - 24	2 - 18	1 - 86	1 - 125	1 - 59	2 - 48	1 - 122	1 - 110	1 - 125
Calcification score for lesions									
Mean ± SD	2.2 ± 1.1	1.7 ± 0.9	1.3 ± 0.6	2.9 ± 1.3	1.9 ± 1.0	2.1 ± 1.1	2.5 ± 1.2	2.4 ± 1.2	2.1 ± 1.1
Calcified lesion thickness (mm)									
Mean ± SD	2.4 ± 0.8	2.3 ± 1.0	3.1 ± 1.2	3.9 ± 1.7	3.1 ± 1.0	3.1 ± 1.0	2.1 ± 0.8	2.0 ± 0.9	2.8 ± 1.3
Range	1 - 4	1 - 4	1 - 5	1 - 8	1 - 5	1 - 5	1 - 4	1 - 5	1 - 8

Table 4 Involvement of the CXCR4/CXCL12 axis in atherosclerosis and arterial injury (modified after (*1,23,24*).

Cell type	Cell type-specific functions
Macrophages	- Up-regulation of CXCR4 by stimulation with oxidized low-density lipoprotein / statins / hypoxia / vascular injury → chemotaxis and enhanced macropinocytosis, modulation of inflammatory phenotype
B- and T-cells	- B-cell development and CXCR4-mediated chemotaxis → pro- / anti-atherogenic effects (phenotype-dependent)
Neutrophils	- CXCR4-maintained homeostasis - CXCR4-regulated neutrophil activation
Platelets	- CXCR4-regulated amplification of platelet activation and platelet survival
Endothelial cells	- Up-regulation of CXCR4 by vascular endothelial growth factor / hypoxia / shear stress - CXCL12/CXCR4 axis-mediated angiogenesis → both detrimental (e.g., plaque neovascularization) and protective effects (e.g., preservation of endothelial barrier function, re-endothelialization)
Vascular smooth muscle cells	- CXCL12/CXCR4 axis-mediated proliferation and migration - CXCR4 up-regulation in the injured arterial wall contributes to intimal hyperplasia → both detrimental (e.g., neointimal hyperplasia) and protective effects (e.g., sustaining a contractile phenotype, plaque-stabilization by fibrous cap formation)

Supplemental Table 1 Results of correlation analysis of ^{68}Ga-Pentixafor PET/CT findings and cardiovascular risk factors.

Cardiovascular risk factor	Number of PET+ lesions		Number of calcified lesions (CT)		TBR	
	r	*P*	*r*	*P*	*r*	*P*
Age at risk	0.60	<0.0001	0.51	0.0001	0.37	0.007
Hypertension	0.56	<0.0001	0.37	0.008	-0.06	0.70
Hypercholesterolemia	0.47	0.0005	0.17	0.24	0.08	0.57
Diabetes mellitus	0.001	0.99	0.05	0.72	0.008	0.96
Smoking history	0.35	0.01	0.20	0.17	0.37	0.008
Male gender	0.05	0.70	0.16	0.27	0.22	0.13
Prior vascular event	0.47	0.0004	0.46	0.0008	0.12	0.40

Supplemental Table 2 Results of multiple regression analysis of ^{68}Ga-Pentixafor PET/CT findings and cardiovascular risk factors.

Cardiovascular risk factor	Number of PET+ lesions		Number of calcified lesions (CT)		TBR	
	r	***P***	***r***	***P***	***r***	***P***
Age at risk	0.50	0.0003	0.49	0.0003	0.32	0.02
Hypertension	0.52	0.0001	-	-	-	-
Hypercholesterolemia	-	-	-	-	-	-
Diabetes mellitus	-	-	-	-	-	-
Smoking history	0.36	0.01	-	-	0.32	0.02
Male gender	-	-	-	-	-	-
Prior vascular event	-	-	0.38	0.008	-	-